Optimum Yield of the Purely Heterogeneous Oxidative Dimerization of Methane

A. J. Colussi[*,1] and V. T. Amorebieta[†]

*Department of Physical Chemistry, Faculty of Exact and Natural Sciences, University of Buenos Aires, 1428-Buenos Aires, Argentina; and
†Department of Chemistry, University of Mar del Plata, P.O. Box 422, 7600-Mar del Plata, Argentina

The optimal C_2-yield per pass for the purely heterogeneous catalytic oxidation of methane by O_2 on Sm_2O_3 under continuous cofeed operation: $\eta_{opt} \leq 0.22 \pm 0.03$, is computed from actual kinetic data for all the pseudoelementary chemical reactions involved. The optimization dispenses with adjustable kinetic parameters, and explores the combined effects of CH_4 and O_2 flow rates, catalyst mass, residence time, and temperature variations on the objective function $\eta = $ methane conversion $\times$ C_2-selectivity for the scheme: CH_4 $(+O_2) \Rightarrow CH_3 (\rightarrow) 1/2C_2H_6 \Rightarrow 1/2C_2H_4 \Rightarrow CO$. The fact that the derived η_{opt} value essentially coincides with the largest C_2-yields reported on a myriad catalysts under vastly different conditions: (1) proves that the ceiling to selectivity is solely determined by the competition among heterogeneous processes and (2) implies a substrate-independent selectivity pattern for the species formed in O_2 dissociative chemisorption. We briefly analyze the physical basis of these propositions and of the prospects of improving C_2-yields beyond 25%. © 1997 Academic Press

INTRODUCTION

The significance of natural gas as a source of energy and materials in the 21st century has prompted renewed interest in basic and applied aspects of methane chemistry (1, 2). The combustion of CH_4, having a lower C : H ratio, releases less CO_2 per unit energy than oil or coal thereby minimizing greenhouse effects. The conversion of methane into more easily transportable liquid fuels is also being actively pursued (3–7).

Reforming methane into synthesis gas, followed by catalytic conversion to methanol is the only method of current commercial value (8). However, the large endothermicity of the first stage and the large capital costs are serious drawbacks that justify seeking for more practical pathways. Controlled oxidation via transition metal catalysis (9), superacid chemistry (1, 10), and methane monooxygenase (11), or its synthetic analogs (12), are promising leads in this direction. Nevertheless, the use of metal oxides as catalysts of methane dehydrogenation remains the method of choice for large volume processing (3b). However, it has proved impossible to break an apparent ceiling to C_2-yields of about 25%, a figure that represents the threshold for an economically viable operation at current prices (13, 14).

Various metal oxides catalyze the partial oxidation of methane into methyl radicals at high temperatures (15, 16). Methyl radicals desorb into the gas-phase, where they self-associate or engage in oxidation reactions (17). Some return to the solid for further oxidation. Ethane and ethylene, the product species of interest, are also oxidized on the catalyst (18). Since methane is the least reactive hydrocarbon under all conditions, a trade-off between conversion and C_2-selectivity is naturally expected. What is at issue is the maximum C_2-yield attainable and—if economically attractive—how to approach it by suitable process design (5, 6, 19, 20).

Recently, two recycling schemes separating the more reactive C_2-products at small ($\approx 3\%$) methane conversions per pass by different strategies have succeeded in reaching 85% yields (21, 22). They may ultimately represent the only viable alternative for implementing the oxide catalyzed conversion of methane. However, and despite much effort, we believe that the basic question of which is the best possible performance in a one-stage continuous cofeed operation—although long surmised—has not been compellingly answered yet.

Previous attempts addressing this important point were confronted with the lack of kinetic data and product distributions for the relevant heterogeneous reactions (5, 6, 23, 24). This fact precludes making genuine predictions because—while the concomitant gas-phase radical chain reactions can be potentially quenched (25, 26)—the heterogeneous oxidation of products and intermediates are intrinsic degradative processes under steady state operation. In this connection, we recently completed detailed kinetic studies on the very low pressure oxidations of methane, methyl radicals, ethane, and ethylene on samaria (27, 28), that provide a dataset uniquely suited for modeling the oxidative dimerization of methane without making ad-hoc assumptions.

[1] E-mail: colussi@nahuel.q1.fcen.uba.ar; colussi@mdp.edu.ar.

In this paper we show that the rather indiscriminate heterogeneous oxidations—in which C_2-species are only about three times more reactive than methane on samaria ca 1000 K—already impose an upper limit to C_2-yields per pass: $\eta_{opt} \leq 0.22 \pm 0.03$, that matches the largest values obtained on different oxides under various conditions (13). This figure, that can only be arrived at by minimizing the extent of free radical reactions, oxidative or otherwise, in the bulk of the gaseous mixture, implies that: (1) radical reactions must have been restricted to the boundary layer or the interstitial voids of the catalyst during optimal operation (4, 23, 24); (2) under such conditions the best catalysts so far investigated appear to have displayed a universal selectivity pattern towards hydrocarbons (13). This seems to be the first time a fundamental, as opposed to an empirical, limit on selectivity based on actual kinetic data is derived for the continuous oxidative dimerization of methane on metal oxides, although Labinger had previously dealt with the case of Mn/MgO in the intermittent redox regime (19, 20). Present analysis also reveals the operational conditions required to systematically reach such limit and points to specific issues deserving further scrutiny, such as the underlying reason for the abnormally large A-factor associated with the heterogeneous oxidation of ethylene on metal oxides (28).

THE MODEL

Throughout, reference is made to the mechanism of Table 1A that includes relevant heterogeneous reactions and equilibria, as well as their kinetic or thermodynamic

TABLE 1A

Kinetic and Equilibrium Parameters for Heterogeneous Oxidations on Samaria

	Reaction	Parameters	Ref.
(1)	$CH_4(g) + O_{s1}$ $\Rightarrow CH_3(g)$	$\log(k_1/cm^{-2}\,s^{-1})^a$ $= (3.73 \pm 0.45) - (4350 \pm 50)/T$	(27)
(2)	$CH_3(g) + O_{s2}$ $\Rightarrow CO_x(g)$	$\log(k_2/k_1)$ $= -(2.18 \pm 0.35) + (3210 \pm 301)/T$	(27)
(3)	$C_2H_6(g) + O_{s3}$ $\Rightarrow C_2H_5(g)$	$\log(k_3/k_1)$ $= -(0.14 \pm 0.30) + (663 \pm 300)/T$	(28)
(4)	$C_2H_4(g) + O_{s4}$ $\Rightarrow CO_x(g)$	$\log(k_4/k_1)$ $= (1.08 \pm 0.35) - (646 \pm 365)/T$	(28)
(I)	$O_2(g) \Leftrightarrow 2O_{s1}$	$\log(K_I/nM^{-1})$ $= (1.89 \pm 0.25) - (4170 \pm 260)/T$	(27)
(II)	$O_2(g) \Leftrightarrow 2O_{s2}$	$\log(K_{II}/nM^{-1})$ $= (5.65 \pm 0.11) - (6480 \pm 130)/T$	(27)
(III)	$O_2(g) \Leftrightarrow 2O_{s3}$	$\log(K_{III}/nM^{-1})$ $= (1.85 \pm 0.22) - (4123 \pm 260)/T$	(28)
(IV)	$O_2(g) \Leftrightarrow 2O_{s4}$	$\log(K_{IV}/nM^{-1})$ $= (5.31 \pm 0.65) - (6480 \pm 647)/T$	(28)

^{a} Determined at very low pressures over 240 mg of Sm_2O_3 exposing a visual area of about 1 cm^2 (see Refs. (27, 28) for further details).

TABLE 1B

Kinetic Parameters for Gas-Phase Reactions^a

	Reaction	Parameters^b
(5)	$CH_3 + CH_3 = C_2H_6$	$\log k_5 = 3.00 - 0.64 \log T$
(6)	$C_2H_5 = C_2H_4 + H$	$\log k_6 = 9.69 + 1.19 \log T - 8131/T$
(-6)	$H + C_2H_4 = C_2H_5$	$\log k_{-6} = -3.08 + 1.49 \log T - 216/T$
(7)	$CH_3 + C_2H_6$ $= CH_4 + C_2H_5$	$\log k_7 = -12.23 + 4.0 \log T - 1810/T$
(8)	$CH_3 + C_2H_4$ $= CH_4 + C_2H_3$	$\log k_8 = -0.20 - 3497/T$
(9)	$H + CH_4 = CH_3 + H_2$	$\log k_9 = -7.75 - 1915/T$
(10)	$H + C_2H_6 = C_2H_5 + H_2$	$\log k_{10} = -9.26 + 3.5 \log T - 1130/T$

^{a} Data taken from Ref. (35), as quoted in Ref. (36a), except for k_8 from Ref. (36b).
^{b} All rate constants in (nM^{-1} s^{-1}) units, except for k_6 in s^{-1}.

parameters on samaria. Table 1B compiles some pertinent gas-phase reactions. We wish to emphasize that our goal is to define the limiting conditions leading to it and to quantify the highest possible C_2-yield via the analysis of an irreducible model of the catalytic oxidation of methane on metal oxides under continuous operation. In other words, we do not attempt to simulate actual experiments (5, 6), a complex and perhaps futile task that demands information on ill-defined features, such as catalyst morphology, mass, and heat transfer parameters, and the spatial interplay of catalytic and gas-phase combustion chemistries. We recognize from the outset that the concentration gradients developing in plug flow over fixed bed reactors would only enhance product oxidation, thereby reducing C_2-yields.

Accordingly, we analyze an isothermal, well-stirred catalytic flow reactor operating at atmospheric pressures. We focus our attention on the composition of the effluent gases at steady state flow conditions. The reactor is fed with methane/oxygen mixtures, diluted in an inert carrier gas if needed. Residence times τ are identical for all species. We use our own data for the reactions of Table 1A (27, 28); the products correspond to the species released to the gas-phase. It can be readily shown that only rate constant ratios (k_x/k_1) are involved in yield optimization. Since the rate constants of steps 1–4 were determined on the same samaria catalyst sample under O_2-chemisorption equilibrium conditions (27, 28), the ratios (k_x/k_1) given in Table 1A are actually independent of catalyst mass, active area, or morphology, thereby eliminating the typical uncertainties associated with catalytic kinetic data transferability. Oxygen consumption is evaluated for an assumed $CO/CO_2 = 1$ stoichiometry in reaction 4; however, it can be shown that other plausible choices do not sensibly affect the results. Considering that the chemisorption equilibria I–IV are maintained by relatively fast reactions (29–31), the ratios (k_x/k_1) are also independent of the possible competition among hydrocarbons for O_s species, i.e., of the composition of the

overhead reaction mixture, except perhaps at very low O_2 partial pressures (32).

Direct experimental evidence indicates that the rates of reactions 1–4 depend on $[O_2(g)]$ according to (27–30, 33),

$$-d[X]/dt = k_x[X]/\left(1 + K_x^{-1/2}[O_2]^{-1/2}\right), \qquad (V)$$

where the k_x's are the rate constants for the pseudoelementary reactions 1–4, and the K_x's are the equilibrium constants for the generation of the participating O_{sx} species. Notice that at atmospheric pressures, gas-phase reactions 5 and (6, -6) are close to their high pressure limits at the temperatures of interest.

YIELD OPTIMIZATION

The set of differential equations describing the kinetics of the different species, that include the corresponding inflow and outflow terms for methane and oxygen, outflow terms for each intermediate and product gas-phase species and that take into account the explicit dependences of rates on $[O_2]$ and temperature (cf. Eq. (V) and Tables 1A, 1B), were integrated by means of the FACSIMILE package (34). The objective function, defined as: $\eta = (2[C_2H_6] + 2[C_2H_4] + [CH_3])/[CH_4]_0$, was initialized at different $\eta < 1$ values and optimized by simultaneously floating some or all of the following parameters: methane and oxygen flow rates, catalyst mass, temperature, and residence time, using the parameter optimization option of FACSIMILE. The algorithm initially evaluates the residual R between the calculated and target η values, and the sensitivity matrix over all adjustable parameters $p_i : \{\partial R/\partial p_i\}$. It then proceeds to minimize R by varying the relevant p_i's, and the cycle is repeated until convergence within a given tolerance is reached.

It is convenient to begin the analysis of the subset of purely heterogeneous oxidations, reactions 1–4 plus reactions 5 and (6, -6). This may seem arbitrary, but the derived results match so closely the highest reported C_2-yields that the exercise turns out to be meaningful (see below). In Fig. 1 we display a representative η vs (residence time, temperature) 3D plot, whereas in Fig. 2 we present the derived η_{opt} values as a function of temperature. We found an upper limit, $\eta_{opt} \leq 0.22 \pm 0.03$, nearly independent of temperature in the interval $800 \leq T/K \leq 1200$. The error bounds are estimated by a sensitivity analysis, in combination with the standard errors of k_3 (10%) and k_4 (30%), derived in Ref. (28). η_{opt} depends inversely on k_3 and k_4 because waste carbon oxides are produced in the oxidation of ethylene rather than in step 2.

We verified that η_{opt} is independent of the number of adjustable parameters, or of their initial values over wide ranges. Of course, η_{opt} is compatible with many different combinations of parameter values. A typical set in a 0.09 L reactor at 1000 K is: residence time = 8.3 s,
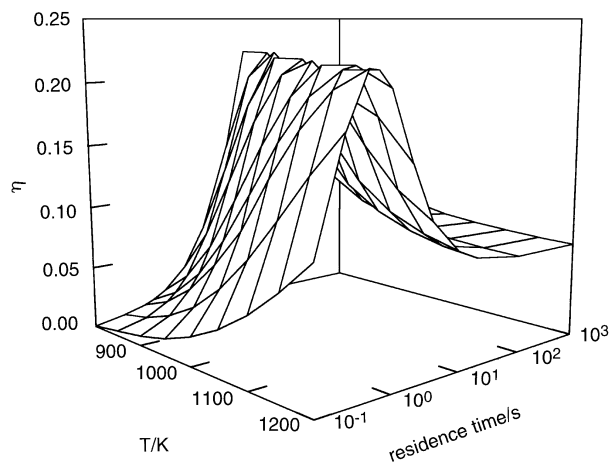

FIG. 1. The calculated yield: $\eta = (2[C_2H_6] + 2[C_2H_4] + CH_3)/[CH_4]_0$, as a function of temperature and residence time τ. Calculations were performed using reactions 1–6, I–IV (Tables 1A, 1B) for a 1:1 CH_4/O_2 mixture, $F_{methane} = F_{oxygen} = 4.5 \times 10^{-4}$ moles/τ, flowing over 240 mg Sm_2O_3 in a 90-cm^3 reactor. Notice that the largest η values along the ridge remain below 0.22.

catalyst mass = 94 mg, $F(CH_4) = 80$ μmoles s^{-1}, $F(O_2) = 108$ μmoles s^{-1}. These conditions lead to 43.7% methane conversion and to a C_2-selectivity of 51%, or $\eta_{opt} = 0.223$. We checked that in this case η already rises to a plateau value of ca 0.20 above $F(O_2) \geq 32$ μmoles s^{-1}, which closely corresponds to a $\Delta(CH_4)/\Delta(O_2) \sim 1$ overall stoichiometry.
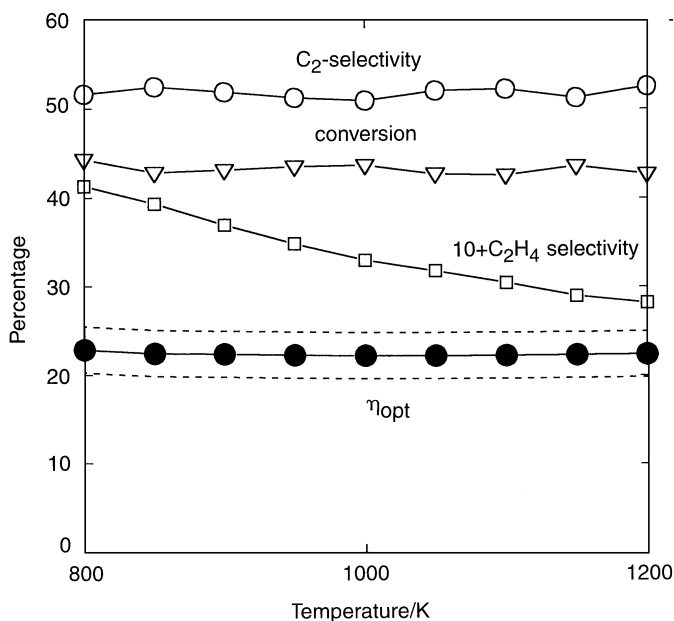

FIG. 2. The optimum yield η_{opt}, methane conversion ($[CH_4]_0 - [CH_4])/[CH_4]_0$, C_2-selectivity $2([C_2H_6] + [C_2H_4])/([CH_4]_0 - [CH_4])$, and ethylene selectivity $2[C_2H_4]/([CH_4]_0 - [CH_4])$, at optimum conditions, expressed as percentages as function of temperature. The dotted lines correspond to the limits imposed by the sum of the propagated standard errors of k_3 and k_4 (see text).

Assuming an active area of ca 10 m^2 g^{-1} for Sm$_2$O$_3$, or about 5×10^{18} active sites m^{-2}, one obtains a turnover number of about 0.6 molecules site^{-1} s^{-1}, which is well within the expected range for a real catalyst (13, 15, 37). Notice that since $K_I = 5.2 \times 10^{-3}$, $K_{III} = 5.3 \times 10^{-3}$, $K_{IV} = 6.8 \times 10^{-2}$ nM^{-1} at 1000 K (from Table 1A), oxidation reaction rates become independent of [O$_2$] above 0.01 Torr (1.33 Pa). In addition, because $K_{IV} > K_{III} \sim K_I$ at all relevant temperatures, the differences between overall rate constants: $k'_x = k_x/(1 + K_x^{-1/2}[O_2]^{-1/2})$ (from Eq. (V)) tend to increase at lower [O$_2$]'s—i.e., $(k'_4 - k'_1) > 0$ is an increasing function of [O$_2$]$^{-1/2}$. Therefore, the largest η values attain at [O$_2$] > 10 K_{IV} at each temperature. The association of methyl radicals at or above atmospheric pressure, step 5, is much faster than their heterogeneous oxidation, step 2, for all sizable conversions. Accordingly, we could reproduce the optimum value: $\eta_{opt} \leq 0.23$, using an even simpler three-reaction skeleton mechanism comprising steps 1, 3, and 4—properly contracted to exclude the implicit intermediacy of CH$_3$ and C$_2$H$_5$ radicals, i.e., CH$_4 \Rightarrow 1/2$C$_2$H$_6 \Rightarrow 1/2$C$_2$H$_4 \Rightarrow$ CO$_x$, with rates proportional to k_1, k_3, and k_4, respectively, and dropping F[O$_2$] as an adjustable parameter.

The fact that gas-phase radical-molecule reactions are apparently unnecessary to reproduce the highest yields obtained in these systems demands a physical explanation. It is essential to realize that if CH$_3$ radicals were uniformly mixed in the reactor volume they would competitively engage in reactions 7 and 8. H-atoms formed in the decomposition of ethyl radicals, reaction 6, would also participate in the fast reactions 9 and 10. We anticipated that the inclusion of the gas-phase reaction of Table 1B would have a deleterious effect on η_{opt} because carbon oxides are largely formed in the heterogeneous oxidation of ethylene, and the net effect of gas-phase radical reactions is to accelerate the conversion of ethane into ethylene.

This contention is clearly confirmed by numerical optimization of an expanded scheme, including steps (7–10): the largest η values never exceed 0.17 (0.167, 0.134, and 0.119 at 800, 1000, and 1200 K, respectively). Therefore, under optimal operating conditions radical–radical reactions, such as step 5, or radical decompositions (viz. step 6) must compete favorably with diffusion away from the vicinity of the catalyst. Although not generally attained, such a regime is expected to prevail in narrow catalyst pores at high pressures of an inert gas (only inert gases will just retard diffusion, because reactants also accelerate gas-phase reactions). Under such conditions the bimolecular recombination of methyl radicals will proceed at rates faster than those estimated from the methyl radical concentrations averaged over the entire reactor volume. Also, during their short ($\sim$1 μs ca 1000 K) lifetime, C$_2$H$_5$ radicals could only diffuse a few μm away from the surface at atmospheric pressures. In this environment, H-atoms formed in reaction 6 will presum-

ably annihilate over the oxidizing catalyst wall rather than participate in activated bimolecular reactions. As a direct consequence of the absence of free radicals in the bulk, the development of oxidative chain reactions will be severely limited (38, 39). McCarty *et al.* have previously argued along similar lines (5). Notice that our zero-dimensional analysis—that does not explicitly consider mass transfer processes—reveals, however, that optimal conditions may involve a conjunction of control variables and morphological features.

The fundamental reason why gas-phase oxidation reactions can only spoil the derived $\eta_{opt} \leq 0.22$ value is that the relative rates: $\rho(HO_2 + X) = r(HO_2 + X)/r(HO_2 + CH_4)$, of HO$_2$ radical reactions—the dominant carrier in branched chain hydrocarbon oxidations (38, 39)—$\rho(HO_2 + CH_3) : \rho(HO_2 + C_2H_6) : \rho(HO_2 + C_2H_4) :: 4.8 \times 10^5 : 11.9 : 10.5$ (35), are much larger than those for the active O$_s$ surface species formed by O$_2$-chemisorption on samaria: $\rho(O_s + CH_3) : \rho(O_s + C_2H_6) : \rho(O_s + C_2H_4) :: 10.7 : 3.3 : 2.7$ at 1000 K (cf. Table 1A). The O$_s$'s are even less selective than the very reactive gas-phase O-atoms, for which the 130 : 3.6 : 13.0 sequence applies at 1000 K (35). In other words, gas-phase oxidation processes, that proceed via more selective intermediates, necessarily decrease the yield of higher hydrocarbons. The availability of experimental rates for the heterogeneous oxidations of all relevant species, measured under identical low-pressure conditions that minimize spurious gas-phase reactions (27, 28), is the crucial information required to reach such a conclusion. Notice the dual, and perhaps confusing, meaning of selective in this context: the more selective radicals attack C$_2$-species much faster than CH$_4$ and lead, therefore, to lower C$_2$-selectivities. It is instructive to consider that the extreme, hypothetical case of truly unselective O$_s$ species toward methane, ethane, and ethylene, i.e., $k_1 = k_3 = k_4$ at all temperatures, with the same stoichiometries of Table 1A leads to $\eta_{opt} = 0.382$. This figure may represent the utmost possible yield over an ideal catalyst under continuous operation.

It is possible to oxidize hydrocarbons on catalysts continuously replenished by electrochemical oxygen transport through Y$_2$O$_3$–ZrO$_2$ membranes, a strategy that effectively segregates the oxidant from the hydrocarbon mixture (26). Other possibilities have also been explored in this regard (25). Thus, it should be realized that the analysis of a continuous oxidative coupling system in which gas-phase radical-molecule reactions are kept to a minimum is not a gedanken experiment, but addresses a tantalizing possibility. Under such conditions the only processes effectively controlling selectivity are heterogeneous oxidations, reactions 1, 3, and 4. Therefore the optimum η_{opt} value derived above for such scenario should be an absolute maximum for samaria as a catalyst. If the presently calculated η_{opt} value were larger than 25%, there would be still room for unprecedented improvements aiming at quenching gas-phase oxidations.

Unfortunately this is not the case, and one must conclude that some experimental studies have unwittingly met the optimal conditions already (13). Our proof, by focusing on an idealized system—that can be, in principle, indefinitely approached by proper experimental design—rather than on an actual experiment, is able to set a hard upper limit on η that does not depend on the details of potentially disposable degradation pathways.

At this stage one cannot help but wonder why the $\eta = 0.25$ boundary has never been crossed on the myriad of tested catalyst oxides other than samaria (13). In this connection, kinetic results are particularly suggestive. Not only activation energies for H-atom abstraction from methane by chemisorbed O_s species are nearly identical on apparently different materials such as Li/MgO (30), Sm_2O_3 (29), and Sr/La_2O_3 (33), but the oxygen activation processes preceding them also bear strong similarities. The appreciably different parameters of the $K_{I–IV}$ equilibrium constants associated with the oxidation of the various hydrocarbons further imply distinguishable O_s species, rather than a single, albeit selective, O_s moiety (27, 28). Moreover, the chemisorptive equilibria I–IV are endothermic and exentropic on all three materials investigated. In other words, the catalytic activity of the oxides becomes less sensitive to oxygen partial pressure at higher temperatures. This behavior can be reconciled with our understanding of gas–solid adsorption if the catalysts cooperate with O_2-chemisorption by concomitant restructuring, thereby compensating for the loss of translational entropy (27, 40, 41). Direct spectroscopic evidence that such restructuring actually takes place in oxidation catalysts such as perovskites is beginning to emerge (42). In other words, catalytic oxides seem to provide a plastic matrix able to incorporate gaseous O_2 and transform it into oxidative centers. Therefore, it is plausible to speculate that the $\eta_{opt} \leq 0.22$ limit derived for Sm_2O_3 is actually a general bound because reflects the selectivity of similar O_s species formed by a common mechanism. This argument, of course, does not rule out the existence of other catalytic materials possessing better characteristics.

On closer inspection, present results reveal that the single critical parameter limiting selectivity in methane oxidative dimerization is the abnormally large A-factor of reaction 4, which is tenfold larger than A_1 or A_3 (cf. Table 1A). Considering that the activation energy of step 4 is larger than E_1 due to a 5 kcal/mol difference in C−H bond energies, the higher reactivity of ethylene—the immediate precursor of waste carbon monoxide—stems from entropic rather than from energetic factors (28). This is consistent with the establishment of an equilibrium binding C_2H_4 on Lewis-basic oxide surfaces prior to its reaction with O_s species (43a), or with a looser transition state for the latter. Apparently, charge transfer processes, that promote O_2 dissociative chemisorption on metal oxides, may also capture ethylene onto their surfaces (43b, 44). We calculate that

decreasing A_4 threefold, which is perhaps within the real possibilities of tailoring oxide catalysts, would improve η_{opt} from 0.22 to 0.32. A $\eta_{opt} \sim 0.3$ yield is already comparable to the performance of the ARCO Mn/MgO catalysts in the discontinuous redox mode (19, 20).

The recognition of a fundamental ceiling to C_2 yields in the oxidation of methane on metal oxides in continuous cofeed flow reactors, justifies the search for alternative schemes. A different approach to enhanced C_2-yields would capitalize, for example, on the different kinetic and thermodynamic parameters associated with the equilibria that generate the various O_s species (27, 28). We have recently shown one way to exploit this advantage: the formation of carbon oxides is considerably delayed relative to the onset of methane oxidation by pulsing CH_4/O_2 mixtures on nonstoichiometric samaria (32).

CONCLUSIONS

Actual kinetic data for the heterogeneous oxidations of methane, ethane, and ethylene on samaria are used to derive a hard upper limit to the yield of C_2-hydrocarbons per pass in the partial oxidation of methane by oxygen on metal oxides under continuous cofeed operation. An optimal value: $\eta_{opt} \leq 0.22 \pm 0.03$, between 800 and 1200 K, confirms and rationalizes a vast body of information and identifies the critical chemical and operational factors controlling selectivity in methane oxidative coupling.

REFERENCES

1. Olah, G. A., and Molnar, A., "Hydrocarbon Chemistry," Wiley, New York, 1994.
2. Crabtree, R. H., *Chem. Rev.* **95**, 987 (1995), and references therein.
3. (a) Keller, G. E., and Bhasin, M. M., *J. Catal.* **73**, 9 (1982); (b) Bhasin, M. M., and Campbell, K. D., *in* "Methane and Alkane Conversion Chemistry" (M. M. Bhasin and D. W. Slocum, Eds.), Plenum, New York, 1995.
4. Kalenik, Z., and Wolf, E. E., "Catalysis, A Specialist Report," Vol. 10, p. 154, Royal Chem. Soc., London, 1993.
5. McCarty, J. G., "Direct Methane Conversion by Oxidative Processes" (E. E. Wolf, Ed.), p. 320, Van Nostrand Reinhold, New York, 1991.
6. McCarty, J. G., McEwen, A. B., and Quinlan, M. A., "New Developments in Selective Oxidation" (G. Centi and F. Trifiro, Eds.), p. 405, Elsevier, Amsterdam, 1990.
7. Hall, R. B., and Myers, G. R., "Symposium on Methane and Alkane Conversion Chemistry, San Diego, CA, March 13–18, 1994."
8. Dry, M. E., *Catal. Today* **6**, 183 (1990).
9. (a) Gardner, K. A., and Mayer, J. M., *Science* **269**, 1849 (1995); (b) Shilov, A. E., "Activation and Functionalization of Alkanes" (C. L. Hill, Ed.), Wiley, New York, 1989.
10. Bucsi, M., and Olah, G. A., *J. Catal.* **16**, 27 (1992).

11. (a) Green, J., and Dalton, H., *J. Biol. Chem.* **264**, 17698 (1989); (b) Dalton, H., Wilkins, P. C., Deighton, N., Podmore, I. D., and Symons, M. C. R., *Faraday Discuss.* **93**, 163 (1992).

12. Barton, D. H. R., and Doller, D., *Acc. Chem. Res.* **25**, 504 (1992).

13. Krylov, O. V., *Catal. Today* **18**, 209 (1993); see in particular Fig. 6, p. 231.

14. Fox, J. M., *Catal. Rev.-Sci. Eng.* **35**, 169 (1993).

15. Otsuka, K., Jinno, K., and Morikawa, A., *J. Catal.* **100**, 353 (1986).

16. Ito, T., Wang, T. X., Lin, C. H., and Lunsford, J. H., *J. Am. Chem. Soc.* **107**, 5062 (1985).

17. Lunsford, J. H., *Langmuir* **5**, 12 (1989).

18. Morales, E., and Lunsford, J. H., *J. Catal.* **118**, 255 (1989).

19. Labinger, J. A., and Ott, K. C., *J. Phys. Chem.* **91**, 2682 (1987).

20. Labinger, J. A., *Catal. Lett.* **1**, 371 (1988). Simulations and limit calculations reported in Refs. (19, 20) correspond to the so-called redox mode, i.e., one in which methane and the oxidant are alternatively fed to the catalyst.

21. Tonkovich, A. L., Carr, R. W., and Aris, R., *Science* **262**, 261 (1993).

22. Jiang, Y., Yentekakis, I. V., and Vayenas, C. G., *Science* **264**, 1563 (1994).

23. Reyes, S. C., Iglesia, E., and Kelkar, C. P., *Chem. Eng. Sci.* **48**, 2643 (1993).

24. Iglesia, E., and Reyes, S. C., Symposium on Methane and Alkane Conversion Chemistry, San Diego, CA. March 13–18, 1994.

25. Lafarga, D., Santamaría, J., and Menéndez, M., *Chem. Eng. Sci.* **49**, 2005 (1994).

26. (a) Vayenas, C. G., Ladas, S., Bebelis, S., Yentekakis, I. V., Neophytides, S., Yi, J., Karavasilis, C., and Pliangos, C., *Electrochim. Acta* **39**, 1849 (1994); Eng, D., and Stoukides, *Catal. Rev. Sci. Eng.* **33**, 375 (1991).

27. Amorebieta, V., and Colussi, A. J., *J. Am. Chem. Soc.* **117**, 3586 (1995).

28. Amorebieta, V., and Colussi, A. J., *J. Am. Chem. Soc.* **118**, 10236 (1996).

29. Amorebieta, V., and Colussi, A. J., *J. Phys. Chem.* **93**, 5155 (1989).

30. Amorebieta, V. T., and Colussi, A. J., *J. Phys. Chem.* **92**, 4576 (1988).

31. Colussi, A. J., and Amorebieta, V. T., *in* "Methane and Alkane Conversion Chemistry" (M. M. Bhasin and D. W. Slocum, Eds.), p. 131, Plenum, New York, 1995.

32. Colussi, A. J., and Amorebieta, V. T., *J. Phys. Chem.* **99**, 13921 (1995).

33. Feng, Y., Niiranen, J., and Gutman, D., *J. Phys. Chem.* **95**, 6558 and 6564 (1991).

34. Curtis, A. R., and Sweetenham, W. P., "FACSIMILE: a computer program for flow and chemistry simulation, and general initial value problems," Harwell, UK. 1987.

35. Baulch, D. L., Cobos, C. J., Esser, C., Frank, P., Just, Th., Kerr, J. A., Pilling, M. J., Troe, J., Walker, R. W., and Warnatz, J., *J. Phys. Chem. Ref. Data* **21**, 411 (1992), as in Ref. (36).

36. (a) Westley, F., Frizzell, D. H., Herron, J. T., Hampson, R. F., and Mallard, W. G., "NIST Chemical Kinetics Database 17, Version 5.0," National Institute of Standards and Technology, Gaithersburg, MD, 1993; (b) Ahonkhai, S. I., Lin, X.-H., and Back, M. H., *Int. J. Chem. Kinet.* **21**, 1 (1989).

37. Boudart, M., *Chem. Rev.* **95**, 661 (1995).

38. Grela, M. A., Amorebieta, V. T., and Colussi, A. J., *J. Phys. Chem.* **96**, 7013 (1992).

39. Grela, M. A., and Colussi, A. J., "Twenty-Fifth Symposium (International) on Combustion/The Combustion Institute, 1994," p. 733.

40. Borg, R. J., and Dienes, G. J., "The Physical Chemistry of Solids," Chap. 10, Academic Press, San Diego, 1992.

41. (a) Somorjai, G. A., *Annu. Rev. Phys. Chem.* **45**, 721 (1994); (b) Levine, R. D., *Catal. Lett.* **9**, 231 (1991); (c) Levine, R. D., and Somorjai, G. A., *Surf. Sci.* **232**, 407 (1990); (d) Amorebieta, V. T., and Colussi, A. J., manuscript in preparation.

42. Gai, P. L., and Kourtakis, K., *Science* **267**, 661 (1995).

43. (a) Aika, K.-I., and Lunsford, J. H., *J. Phys. Chem.* **82**, 1794 (1978). (b) Gates, B. C., "Catalytic Chemistry," p. 392, Wiley, New York, 1992, and references therein.

44. Amorebieta, V. T., and Colussi, A. J., We recently found that ethylene decays autocatalytically by reaction with oxygen vacancies in partially reduced samaria samples.